

# Portrait3D: 3D Head Generation from Single In-the-wild Portrait Image

Jinkun Hao<sup>1</sup>, Junshu Tang<sup>1</sup>, Jiangning Zhang<sup>2</sup>, Ran Yi<sup>1†</sup>, Yijia Hong<sup>1</sup>, Moran Li<sup>2</sup>  
 Weijian Cao<sup>2</sup>, Yating Wang<sup>1</sup>, Lizhuang Ma<sup>1†</sup>  
<sup>1</sup>Shanghai Jiao Tong University, <sup>2</sup>Youtu Lab, Tencent

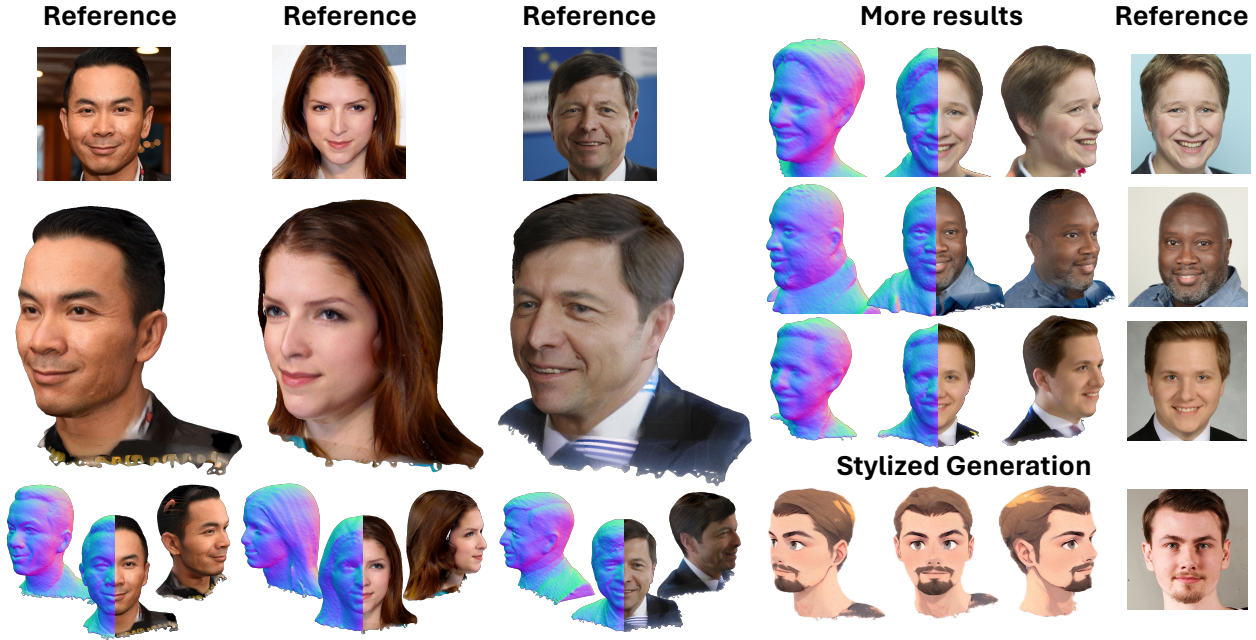


Figure 1. Given an in-the-wild portrait image, Portrait3D has the ability to generate high-quality 3D head with detailed face geometry and photo-realistic texture. With stylized diffusion models, Portrait3D can be used to customize 3D heads with multiple styles while keeping the identity in the portrait image.

## Abstract

While recent works have achieved great success on one-shot 3D common object generation, high quality and fidelity 3D head generation from a single image remains a great challenge. Previous text-based methods for generating 3D heads were limited by text descriptions and image-based methods struggled to produce high-quality head geometry. To handle this challenging problem, we propose a novel framework, **Portrait3D**, to generate high-quality 3D heads while preserving their identities. Our work incorporates the identity information of the portrait image into three parts: 1) geometry initialization, 2) geometry sculpting, and 3) texture generation stages. Given a reference portrait image, we first align the identity features with text features to realize ID-aware guidance enhancement, which contains the control signals representing the face information. We then use the canny map, ID features of the portrait image, and

a pre-trained text-to-normal/depth diffusion model to generate ID-aware geometry supervision, and 3D-GAN inversion is employed to generate ID-aware geometry initialization. Furthermore, with the ability to inject identity information into 3D head generation, we use ID-aware guidance to calculate ID-aware Score Distillation (ISD) for geometry sculpting. For texture generation, we adopt the ID Consistent Texture Inpainting and Refinement which progressively expands the view for texture inpainting to obtain an initialization UV texture map. We then use the id-aware guidance to provide image-level supervision for noisy multi-view images to obtain a refined texture map. Extensive experiments demonstrate that we can generate high-quality 3D heads with accurate geometry and texture from a single in-the-wild portrait image. The project page is at <https://jinkunhao.github.io/Portrait3D/>.

<sup>†</sup>Corresponding authors.

# 1. Introduction

3D head generation aims at creating high-quality 3D digital assets of human heads that align with user preferences utilizing various input data, which has significant application in film character creation, gaming, online meetings, education, etc. Conventional methods rely on multi-view geometric consistency [19, 27, 28, 46, 51] or statistical 3D face prior model [2, 10, 52] to achieve high-quality 3D head generation. The former necessitates multi-view images or several minutes of monocular video, which are not applicable to a single in-the-wild portrait image. Moreover, 3D face shape prior models typically focus on the face region, failing to accurately reconstruct the entire head shape and being unable to handle elements such as long hair and clothing. An alternative approach involves employing Generative Adversarial Networks (GANs) to accomplish 3D head generation, which is constrained by limited training data and typically produces frontal-facing faces. Moreover, they struggle to preserve identity consistency when presented with images of large head poses. Recently, text-to-image [14, 29, 32, 33, 37, 38] generation models trained on massive-scale image datasets have achieved significant success. Some approaches employ SDS loss [30] to ensure similarity between the generated 3D model and images, facilitating image-to-3D [23–26, 42] or text-to-3D [21, 30, 39, 43, 44]. However, when employing these methods for customized 3D head generation, the absence of identity information makes it difficult to accurately reproduce the geometric details and texture realism of the head in the portrait image.

Through analyzing previous methods, we summarize the key challenges from the three stages in the optimization-based 3D head generation approach: **1) Geometry Initialization**: Previous image-to-3D methods used an ellipsoid as the initial geometry [5] and could not accurately reconstruct the geometry of the head. On the other hand, text-to-head methods used a unified FLAME head [13, 22] as the geometric prior, which lacks personalized information and cannot generate individualized features that deviate from the FLAME head, such as long hair. **2) Geometry Sculpting**: Although image-to-3D methods attempted to use view-dependent diffusion [23] to guide geometry generation, the resulting geometry lacked the generalization ability to the detailed head geometry. Besides, text-to-3D methods use facial image description text to generate geometry, which can result in a deviation from the identity of the reference image. **3) Texture Generation**: Previous methods used VSD loss [44] to mitigate color over-saturation issues based on SDS. However, the generated textures still tended to have excessive shading and unrealistic texture [16, 22].

To address the challenges mentioned above, we incorporate identity information into the three stages of 3D head generation compared with previous methods 2. Firstly, we

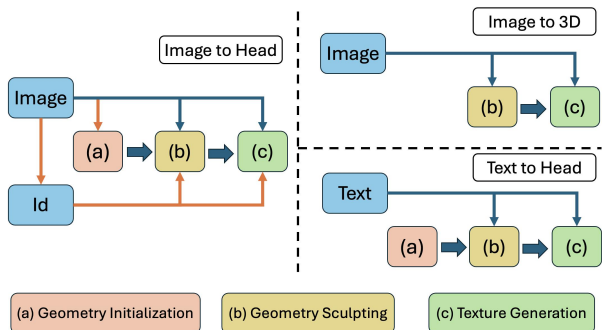


Figure 2. Comparison of previous optimization methods (Right) with our method (Left). Our method leverages the portrait image to get a better initial mesh and utilizes extracted identity information to enhance geometric and texture optimization.

extract Identity embedding using an ID feature extractor and align them with text embedding using a pre-trained ID adapter with decoupled cross-attention. This, along with landmark-guided ControlNet, enables ID diffusion and provides **ID-aware guidance**, allowing us to incorporate the identity and facial layout information from the reference image into the geometry and texture generation stages. Secondly, we propose **ID-aware geometry supervision**. By extracting canny maps containing detailed information from the portrait image, we combine canny-guided ControlNet and ID features with off-the-shelf text-to-normal and text-to-depth methods [16] to generate high-quality geometric constraint for the geometry generation stage. Additionally, we obtain **ID-aware initialization** using 3D GAN inversion. In the geometry sculpting stage, we optimize the 3D head using ID-aware guidance with ID-aware Score Distillation (ISD) loss. In the texture generation stage, we first use Progressive Texture Inpainting to generate a UV-textured map for the uncolored 3D head mesh. Then we leverage ID diffusion to denoise the rendered image from random viewpoints and further refine the texture by calculating the loss between the rendered and denoised images at the image level.

In this paper, we propose Portrait3D, a new method for generating high-quality 3D heads from single in-the-wild portrait images. We present Identity-aware Head Guidance and Initialization (§4.1) and use ID-aware guidance to guide Geometry Generation (§4.2). In the texture generation stage, we propose ID Consistent Texture Inpainting and Refinement (§4.3), where we first use the inpainting approach to generate a rough texture and then use ID-aware guidance for texture refinement. With these methods, we can generate high-quality 3D head models with consistent identities from a single in-the-wild portrait image and further enable texture editing.

In summary, the contributions of our work are as follows:

- A novel pipeline for generating high-quality 3D head

models from a single in-the-wild face image.

- A method that incorporates identity information into the geometry initialization, geometry generation, and texture generation stages, significantly improving the identity details of the generated 3D heads.
- An ID Consistent Texture Inpainting and Refinement method, which uses Progressive Texture Inpainting and refinement approach to achieve photo-realistic texture generation.

## 2. Related work

### 2.1. 3D Head Generation

Recently, various approaches have explored reconstructing 3D head avatars from monocular face videos using different 3D representations. Among these approaches are mesh-based techniques like NHA [10], neural implicit representation such as NerFace [9], explicit point cloud methods like PointAvatar[52], and 3D Gaussian-based approaches like [45]. However, these methods necessitate several minutes of video input and are unable to reconstruct complete heads from single in-the-wild images. Moreover, they struggle to reconstruct less prominent parts in videos, such as the back of the head. In addition, generating heads from 3D GANs has rapidly developed. EG3D [3] proposed a hybrid tri-plane representation that can quickly and efficiently render high-quality facial images. Panohead [1] expanded on EG3D by increasing the number of planes, allowing for the generation of 3D faces from limited angles to the entire head. However, these methods are limited by the representation capability of implicit representation and cannot produce high-quality surface geometry.

With the development of text-to-image models, generating human heads directly from text has become an important application. Headsculpt [13] incorporates facial landmark information into the text-to-3D generation method, effectively constraining the facial layout and avoiding the Janus face problem. HeadArtist [22] builds on Headsculpt by proposing SSD loss and decoupling the geometry and texture generation processes, resulting in an even higher-quality human head generation. Additionally, Humannorm [16] fine-tunes the diffusion model on 3D human body datasets to obtain diffusion models for text-to-normal and text-to-depth, enhancing the generation ability of human body parts. However, the texture generated by these methods can be oversaturated, making it difficult to achieve photo-realistic head generation.

### 2.2. Text to 3D Generation

Recent advances in combining 3D generative architectures with image generative models make it possible to synthesize diverse high-fidelity 3D scenes and objects from text prompts. Efforts such as DreamFusion [30] explore text-

to-3D generation by leveraging a Score Distillation Sampling (SDS) loss derived from a 2D text-to-image diffusion model and show impressive results. Subsequently, based on the promising SDS loss, Magic3D [21] increases the rendering resolution of generated 3D objects from 64 to 512. Fantasia3D [5] models the appearance via the BRDF modeling, generating compelling geometry and photorealistic object texture. ProlificDreamer [44] proposes Variational Score Distillation (VSD), an advanced guiding loss capable of solving oversaturation problems. Although many works have solved the problem of texture oversaturation to some extent, it is still difficult to generate realistic geometry and texture.

### 2.3. Image to 3D Generation

Image-driven 3D generation have also been greatly influenced by the emergence of diffusion models. Zero-1-to-3 first proposes view-dependent diffusion, which primarily focuses on learning camera viewpoints within large-scale diffusion models, enabling zero-shot novel view synthesis. GeNVS [4] leverages pixel-aligned features from input views to add 3D awareness to 2D diffusion models. On the other hand, some optimize-based image-to-3D methods, such as Magic123 [31] and Make-it-3D [42], incorporate 3D priors from Zero-1-to-3 and employ coarse-to-fine two-stage optimization. Make-it-3D, in particular, enhances texture and geometric structure in its fine stage, yielding high-quality textured point clouds as final outputs. Subsequent works [41, 48] have consistently aimed to build upon these achievements, further refining and enhancing the quality of generated 3D models. However, these methods are limited by the ability of view-dependent diffusion, which cannot accurately generate the geometry from the image.

## 3. Preliminaries

**Score Distillation Sampling for 3D Generation.** Recently, optimization based 3D generation approaches usually optimize a 3D scene using Score Distillation Sampling (SDS) [30] loss.

SDS loss is proposed to distillate 3D prior from 2D pretrained diffusion models by minimizing the rendering errors from an optimized 3D scene. Specifically, during optimization, an image  $x_0 = \mathcal{G}(\theta, c)$  is rendered from a 3D representation with parameter  $\theta$  under the randomly sampled camera  $c$  using a differentiable renderer  $\mathcal{G}$ . The SDS loss can be calculated as:

$$\nabla_{\theta} L_{\text{SDS}} = \mathbb{E}_{t, \epsilon} [\omega(t) \|\epsilon_{\phi}(x_t, t, y) - \epsilon\|^2], \quad (1)$$

where  $\omega(t)$  is a weighting function.  $x_t$  is the noisy image by adding noise  $\epsilon \sim \mathcal{N}(0, 1)$  to rendered image  $x_0$  at timestep  $t$ .  $y$  is the conditioned text prompt.  $\epsilon_{\phi}(\cdot)$  is the denoising direction predicted by the pretrained diffusion model  $\phi$ .

SDS encourages creating plausible 3D models that conform to the conditional distribution in diffusion latent space. To improve the geometry quality, the classic SDS loss uses a large weight of classifier-free guidance, which will result in high color saturation.

**Different Variations of SDS.** Recent works [31, 41, 44] introduce different variations of SDS to enhance generation fidelity and training fidelity. Specifically, [44] proposed the Variational Score Distillation (VSD) to improve the texture and geometry quality. VSD treats the 3D optimization process as learning a 3D distribution rather than a single point under the conditional text prior. During the optimization, VSD relies on fine-tuned low-rank adaptation (LoRA) [15] model to represent the distribution of rendered images under different camera poses.

The gradient of  $L_{\text{VSD}}$  could also be approximated as:

$$\nabla_{\theta} L_{\text{VSD}} = \mathbb{E}_{t, \epsilon, c} [\omega(t) \|\epsilon_{\phi}(\mathbf{x}_t, t, y) - \epsilon_{\text{lor}\alpha}(\mathbf{x}_t, t, y, c)\|^2], \quad (2)$$

where  $\epsilon_{\text{lor}\alpha}$  estimates the denoising direction produced by the customized LoRA model. VSD loss effectively improves the fidelity of both texture and geometry.

Based on VSD, DreamCraft3D [41] proposed bootstrapped score distillation (BSD), which personalizes the generative 3D prior by leveraging multi-view renderings of the 3D scene to finetune the pretrained diffusion model:

$$\nabla_{\theta} L_{\text{BSD}} = \mathbb{E}_{t, \epsilon, c} [\omega(t) \|\epsilon_{\text{fit}}(\mathbf{x}_t, t, y) - \epsilon_{\text{lor}\alpha}(\mathbf{x}_t, t, y, c)\|^2], \quad (3)$$

where  $\epsilon_{\text{fit}}$  denotes the finetuned model.

However, the customization for each text-conditioned 3D scene or image is time-consuming. As for optimizing 3D heads, we directly apply a pretrained ID-aware diffusion model as a strong 3D guidance for in-the-wild human heads.

## 4. METHOD

In this paper, we propose Portrait3D, a novel optimization-based pipeline for high-fidelity 360-degree head generation from a single portrait image. We fully leverage state-of-the-art identity-aware priors to our generation process through **ID-aware Initialization**, **ID-aware Guidance**, and **ID-aware Geometry Supervision** (§4.1). The overall pipeline of Portrait3D is shown in Figure 3, which consists of two stages: geometry sculpting stage and texture generation stage.

In the geometry sculpting stage, we utilize DM Tet [40] as the 3D representation and propose **ID-aware Score Distillation (ISD) loss** to inject identity guidance for the optimization (§4.2). Then in the texture generation stage, we propose **ID-Consistent Texture Inpainting and Refinement** for realistic appearance generation (§4.3).

### 4.1. ID-aware Initialization and Guidance

Given a facial image  $\mathbf{x}_{\text{ref}}$  as input, our goal is to generate a high-fidelity 3D head model parameterized with  $\theta$ , that preserves the identity and appearance of the person in the image. We adopt an optimization-based pipeline, and formulate the optimization process for generating 3D head as follows:

$$\begin{aligned} \min \quad & \begin{cases} \mathbb{E}_{t, c} [\text{D}_{\text{KL}}(q_t^{\theta}(\mathbf{x}_t | \mathbf{c}) \| p_t(\mathbf{x}_t | y))], & \mathbf{c} = \mathbf{c}_{\text{rand}} \\ D(\mathbf{x}_{\text{ref}}, g(\theta, \mathbf{c})), & \mathbf{c} = \mathbf{c}_{\text{ref}} \end{cases} \quad (4) \\ \text{s.t.} \quad & \theta = \{\theta | \mathbf{x}_{\text{ref}}, \theta_0\}, \quad \theta_0 = \text{Initial Mesh} \end{aligned}$$

where  $\mathbf{c}_{\text{rand}}$  is a random camera pose, and  $\mathbf{c}_{\text{ref}}$  is the reference camera pose (in  $\mathbf{x}_{\text{ref}}$ ).  $D(\cdot)$  denotes the distance function, and  $\theta_0$  is the initial 3D mesh provided by users, which is usually an ellipsoid or a parametric model.

For 3D full head generation, the quality of the generated 3D head largely relies on the quality of the initial 3D model and the multi-view guidance. Some existing 3D generation methods use text prompts  $y$  that accurately describe the facial image or view-dependent diffusion models [13, 16, 23, 25] to provide additional guidance of the image. However, for one-shot 3D head generation tasks, text prompts can only express limited information:

The direct description of the input facial image, often cannot fully capture the variations of different facial features. Besides, pretrained 2D view-dependent diffusion models (e.g., Zero-123 [23]) are trained on general objects, which often lack the ability to generalize to human heads.

Therefore, our key insight is to fully leverage identity knowledge and inject state-of-the-art identity priors into the mesh initialization and diffusion guidance.

**ID-aware Initialization.** The initialization is crucial for 3D generation. According to the optimization goal in Eq.(4), a good initial 3D mesh  $\theta_0$  should possess the approximate geometric shape of the face in the given image  $\mathbf{x}_{\text{ref}}$ . Some approach uses FLAME [8] to obtain the initial 3D head shape. However, this approach cannot generate personalized facial features and does not describe the geometric shape of hair. To address this issue, we employ a 3D-aware GAN model [1] trained on a comprehensive 360° head dataset to obtain the initial 3D head mesh  $\theta_0$ . Specifically, given the input facial image  $\mathbf{x}_{\text{ref}}$ , 1) we first perform inversion by optimization based on pixel-wise  $\mathcal{L}_2$  loss and image-level LPIPS loss [50], to find the corresponding latent code  $z$ ; 2) and then perform Pivotal Tuning Inversion (PTI) [36], which uses the initial inverted latent code  $z$  as a pivot and finetunes the generator, to obtain a 3D representation that better matches the input image. Through 3D GAN inversion, we can obtain an initial 3D head mesh that corresponds to the input facial image, denoted as:

$$\theta_0 = \text{3D-GAN}(z_0 | \mathbf{x}_{\text{ref}}). \quad (5)$$

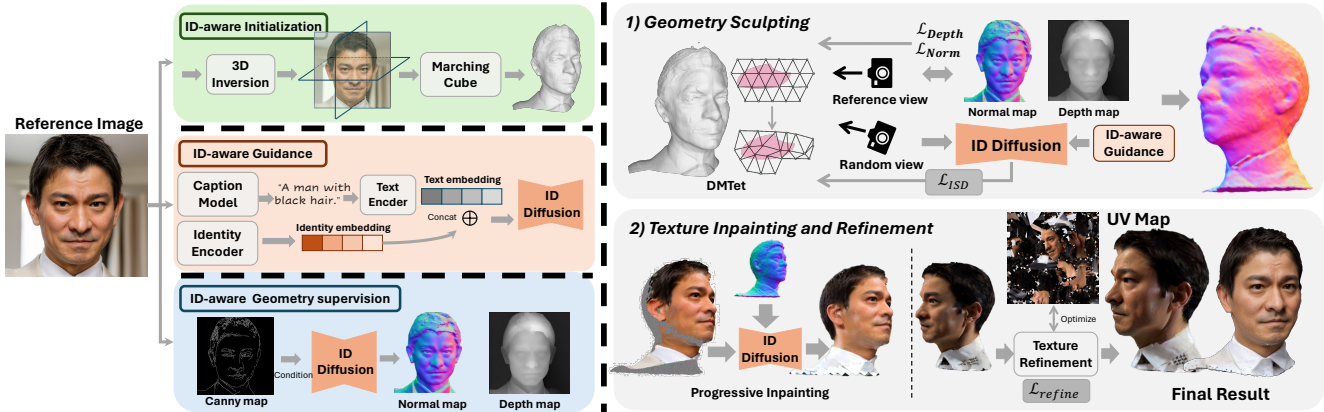


Figure 3. Overview of our proposed Portrait3D framework. Given a single in-the-wild face image, Portrait3D uses Identity-aware Head Guidance and Initialization (§4.1) to integrate identity information into the Geometry Sculpting stage (§4.2). In the texture generation stage, ID Consistent Texture Inpainting and Refinement (§4.3) is applied to generate a high-quality head texture, where we first use the inpainting method to generate a rough texture and then use image-level ID-aware supervision for texture refinement. With these methods, we can generate high-quality 3D head models with consistent identities from a single in-the-wild face image.

**ID-aware Guidance.** In order to obtain finer information about the facial image, we extract high-dimensional identity features  $I_r$  from the reference image as additional conditions beyond text prompt, to guide the denoising process of diffusion models. We use a facial recognition model [6] trained on large-scale facial datasets as the identity encoder to extract robust identity features. Additionally, we utilize a light projection network to map the extracted ID feature to an enhanced ID feature  $f_{ID}$  aligned with text embedding, and insert the ID feature into diffusion with decoupled cross-attention [47]. In this way, we construct an ID-guided diffusion model  $p_t^{id}$ , which will be utilized in our ID-aware SDS loss to provide identity guidance for a specific person.

The aforementioned identity-enhanced prompt only extracts general identity information, but cannot provide the information of facial layout. For example, a person has different mouth shapes when laughing and crying, but the identity features are the same. Therefore, solely using the identity feature-based guidance may lead to inconsistency in the facial layout when viewed from different camera viewpoints. To address this issue, we utilize a pretrained facial shape predictor [11] to obtain 3D facial landmarks of the reference image  $x_{ref}$ , and apply pose alignment to align the 3D facial landmarks to the initial 3D head mesh. Then, given a camera pose  $c$ , we project the extracted 3D facial landmarks onto the 2D plane, and obtain a facial landmark image  $L(c)$ , which provides the facial component layout information from that viewpoint. We then apply a landmark-guided ControlNet [49] to introduce the facial landmarks information into our ID-aware SDS loss. Since the facial landmark images under different viewpoints are projected from the same 3D facial landmarks, they are geometrically consistent. Incorporating these facial landmark images in

our ID-aware SDS will provide multi-view geometry consistency constraints and guidance.

By incorporating three types of information, *i.e.*, text prompt  $y$  (obtained from  $x_{ref}$  by BLIP-2 [20]), identity feature  $f_{ID}$ , and the projected facial landmark image  $L(c)$ , we propose **ID-aware Score Distillation (ISD)** loss, which can be formulated as:

$$\mathcal{L}_{ISD} = \mathbb{E}_{t,c} [D_{KL}(q_t^\theta(x_t|c) || p_t^{id}(x_t|y, f_{ID}, L(c), c))]. \quad (6)$$

Compared to SDS, ISD introduces more ID-preserved supervision that is aligned with the reference portrait image.

**ID-aware Geometry Supervision.** In the geometry sculpting stage, the reference image  $x_{ref}$  in RGB space cannot be directly used as the supervision for geometry. A common method is to use normal maps and depth maps that contain geometric information for supervision, which can be predicted based on the reference image in RGB space. Therefore, it is crucial to obtain high-quality geometric representations  $X_{ref}^{geo}$  from the reference image in RGB space. Previous methods [7] directly predicted depth maps and normal maps from images but failed to capture some geometric details in the reference images, which could result in flat geometries, as shown in Fig 4. Different from previous methods, we first use an edge extractor to extract high-frequency facial geometric details and obtain a Canny image as the condition. Then we utilize pre-trained Text-to-Normal and Text-to-Depth diffusion models [16] with ControlNet to generate normal maps and depth maps. Additionally, to better preserve identity information, we also add ID features into the diffusion process. Through these approaches, high-quality geometric supervision in the refer-

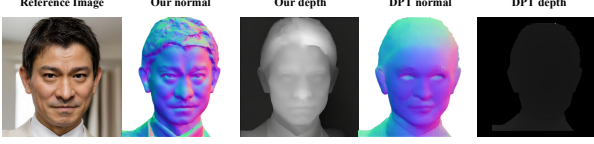


Figure 4. Comparison between our normal map and depth map and those generated by DPT[34, 35].

ence view can be formulated as:

$$\mathbf{X}_{\text{ref}}^{\text{geo}} = p_{\text{geo}}^{\text{id}}(\mathbf{x}_t|y, f_{\text{ID}}, \text{Canny}(\mathbf{x}_{\text{ref}})), \quad (7)$$

where  $\mathbf{X}_{\text{ref}}^{\text{geo}} = \{\mathbf{X}_{\text{ref}}^{\text{normal}}, \mathbf{X}_{\text{ref}}^{\text{depth}}\}$  and  $p_{\text{geo}}^{\text{id}} = \{p_{\text{normal}}^{\text{id}}, p_{\text{depth}}^{\text{id}}\}$ . In this way, the 3D head model can obtain geometric details that are as rich as the information in the RGB image of the reference view.

## 4.2. Geometry Sculpting

During the geometry sculpting stage, we aim to obtain a fine-grained 3D geometry, that is consistent with the facial features in the input image under the reference view, and consistent across different viewpoints. We first convert the initial 3D mesh obtained from ID-aware initialization into a textured 3D mesh representation. In this process, we use deformable tetrahedral grid (DMTet) [40] as the 3D representation to facilitate high-resolution details and high-quality surface. Specifically, we use the normals rendered from 3D-GAN as the pseudo ground truth normals  $\mathcal{N}_{\text{c}}$ . For the DMTet object to be optimized, we use Marching Tetrahedra to generate the normal map  $\hat{\mathcal{N}}_{\text{c}}$ . In order to polish the overall surface from multiple viewpoints, we uniformly sample camera poses  $\mathbf{c}$  distributed in the 3D-GAN space, and use  $\mathcal{L}_2$  distance between normal maps as the loss function, defined as  $\mathcal{L}_{\text{norm}} = \|\hat{\mathcal{N}}_{\text{c}} - \mathcal{N}_{\text{c}}\|_2$ .

**Geometry Refinement.** During the geometry refinement stage, we use **ID-aware Geometry Supervision** (Sec. 4.1) to ensure the generation of fine geometry under the reference view, while supplementing the information with the prior of the diffusion model under other views, as shown in Eq.(4). Under the reference view, we calculate the reference loss from the head foreground mask, normal map, and depth map of the reference image, which is defined as:

$$\mathcal{L}_{\text{ref}} = \mathcal{L}_{\text{mask}} + \mathcal{L}_{\text{normal}} + \mathcal{L}_{\text{depth}}, \quad (8)$$

where the foreground mask  $M$  is obtained through face parsing, and both the mask loss  $\mathcal{L}_{\text{mask}}$  and normal loss  $\mathcal{L}_{\text{normal}}$  are defined as the  $\mathcal{L}_2$  distance between the rendered mask and normal map, and the reference mask and normal map. For the depth loss  $\mathcal{L}_{\text{depth}}$ , we use the negative Pearson correlation to alleviate the problem of depth scale mismatch.

For other views that are randomly sampled around the 3D head, we use the ISD loss  $L_{\text{ISD}}$  in Eq.(6) to guide the

optimization of the geometry, based on the ID-enhanced diffusion prior. Finally, the Marching Tetrahedra algorithm is applied to extract the mesh.

## 4.3. ID-Consistent Texture Inpainting and Refinement

After obtaining a fine-grained 3D geometry in the geometry sculpting stage, during the texture generation stage, our goal is to rapidly generate realistic textures for the 3D head mesh. Previous texture generation methods [5, 44] often used SDS/VSD loss for multi-view optimization to obtain textures. However, the textures generated in this way may become over-saturated and inconsistent with the color tone of the reference image.

Therefore, we design an inpainting and refinement process to quickly produce high-quality UV texture maps without involving SDS/VSD optimization.

**Progressive Texture Inpainting.** With an uncolored 3D head surface mesh  $M$  with vertices  $V$  and triangular faces  $F$  generated in the geometry generation stage, denoted as  $M = (V, F)$ , we initialize a UV texture map  $\mathbf{T}_0$  corresponding to the mesh coordinates. Starting from the reference view  $\mathbf{c}_0$ , we first back-project the reference portrait image onto the 3D mesh. In order to maintain consistency with the reference image texture, we sample a camera trajectory  $\{\mathbf{c}_1, \mathbf{c}_2, \dots, \mathbf{c}_n\}$  (where  $\mathbf{c}_i$  is the  $i$ -th viewpoint, and  $n$  is the number of sampled viewpoints) to progressively generate texture information. The camera trajectory starts from the reference image viewpoint, gradually moves the camera pose to the back view of the head, and finally generates the texture for the top of the head that has not been generated yet.

During the inpainting process, at a specific viewpoint  $\mathbf{c}_k$ , given the texture map  $\mathbf{T}_{k-1}$  that has been textured in  $k-1$  previous viewpoints, we are able to render an RGB image  $I_k$  with partially colored regions, as well as a mask  $\mathbf{m}_{k-1}$  indicating the colored (visible) regions. To better inpaint the uncolored areas, we render a normal map  $\mathbf{x}_k^{\text{normal}}$  from the 3D mesh as the geometric condition at the  $\mathbf{c}_k$  viewpoint, and then use the normal-conditioned diffusion model to generate the texture for the uncolored areas, which can be formulated as:

$$\hat{I}_k = p_0^{\text{id}}(\mathbf{x}_0|y, f_{\text{ID}}, \mathbf{x}_k^{\text{normal}}). \quad (9)$$

The generated image  $\hat{I}_k$  at the viewpoint  $\mathbf{c}_k$  will be projected back onto the 3D mesh, resulting in the inpainted texture map  $\hat{\mathbf{T}}_k$ . And the uncolored region  $(1 - \mathbf{m}_{k-1})$  in UV texture  $\mathbf{T}_{k-1}$  is updated as follows:

$$\mathbf{T}_k = \mathbf{m}_{k-1} \odot \mathbf{T}_{k-1} + (1 - \mathbf{m}_{k-1}) \odot \hat{\mathbf{T}}_k, \quad (10)$$

where  $\mathbf{T}_k$  is the updated UV texture map after  $k$  step inpainting. With this progressive inpainting method, we can gradually inpaint the textures from other viewpoints starting from the reference portrait image.

**Texture Refinement.** Although the UV texture map obtained through texture inpainting may exhibit inconsistent textures in some regions, it provides us with a good texture initialization. In the texture refinement stage, we aim to solve the texture inconsistency problem and further enhance the detail and realism of the generated texture.

We optimize the UV texture map by utilizing the ID-guided diffusion model (Sec. 4.1) and minimizing the distance between the rendered multi-view images and the refined images.

Specifically, for a rendered image  $x_0$  from a sampled viewpoint, we add Gaussian noise with  $t$  diffusion steps and use the ID-guided diffusion model  $p^{id}$  to restore it. Moreover, we add rendered normals  $x^{normal}$  from the corresponding viewpoint as additional geometric information conditions during the diffusion denoising process. This yields a refined image  $\hat{x}_0$  in the respective viewpoint which we will use as supervision to optimize the texture map:

$$\hat{x}_0 = p_0^{id}(x_0|x_t, y, f_{ID}, x^{normal}) \quad (11)$$

After obtaining the refined image  $\hat{x}_0$ , we calculate the pixel-level MSE loss  $\mathcal{L}_{MSE}$  between  $x_0$  and  $\hat{x}_0$  to further refine the texture map. Besides, we add a perceptual loss  $\mathcal{L}_{percep}$  to enhance the texture detail information and maintain style similarity. We also calculate the MSE loss  $\mathcal{L}_{MSE}^{ref}$  between  $x_0$  from the reference view and the reference image  $x_{ref}$ . By combining these supervisions, we obtain the final loss  $\mathcal{L}_{refine}$  for the texture refinement stage:

$$\mathcal{L}_{refine} = \mathcal{L}_{MSE} + \mathcal{L}_{percep} + \mathcal{L}_{MSE}^{ref}. \quad (12)$$

## 5. EXPERIMENT

In the experimental section, we will start with the implementation details, followed by quantitative and qualitative comparisons between our method and others. Finally, we will analyze the role of each module in our method.

### 5.1. Implementation Details

Our Portrait3D is built upon the open-source project ThreeStudio [12]. In the geometry stage, we use SD1.5 [37] as the base diffusion model. During the texture generation stage, we employ Realistic Vision 4.0 as the base diffusion model, which is a version fine-tuned for real portraits on SD1.5. We set the resolution of DM Tet to 512 to achieve better geometric details. Additionally, the size of the unfolded texture map from the mesh is set to 1024x1024. In the geometry generation stage, we perform 5,000 optimization iterations. During the texture generation stage, we first perform texture inpainting from 15 ordered viewpoints, followed by 400 steps of texture refinement. Our experiments are conducted on a machine with a single V100 GPU, with a batch size set to 1. For each 3D head, the total optimization time is approximately 1 hour.

**Baselines.** We conducted extensive comparisons with four other single-view 3D generation methods (Magic123[31], DreamCraft3D[41], Wonder3D[25]) and a single-view human head generation method (Panohead[1]). For Magic123, DreamCraft3D, and Wonder3D, we generated the 3D models strictly following the official open-source code and parameters. For Panohead, we followed the official guidance and obtained results using the GAN inversion method. In addition, we compared our method with the text-to-3D human head generation methods. For a fair comparison, we did not choose the non-open-source methods HeadSculpt[13] and HeadArtist[22]. Instead, we selected the state-of-the-art approach, HumanNorm[16], for it has excellent generation results, open-source code, and good reproducibility.

**Datasets.** We conducted experiments on a subset of facial images from the FFHQ [17] dataset, a high-quality in-the-wild facial dataset known for its rich diversity in age, ethnicity, and image backgrounds, as well as significant variations in facial attributes. This dataset presents a challenging task due to its unconstrained environment. From this dataset, We selected 106 portrait images with unoccluded faces to evaluate our model and baselines.

**Evaluation metrics.** We employ three commonly used metrics to assess the rendered images of the generated heads in terms of image quality and facial reconstruction. LPIPS [50] is utilized for fidelity measurement, while CLIP-I [47] score and ID [1] score are employed to gauge the multi-view consistency and identity preservation.

### 5.2. Qualitative Evaluation

**Qualitative evaluation with image-to-3d methods.** In Fig.5 we show the comparisons between our method and four other image-to-3D methods. These four images are selected from the in-the-wild face image dataset FFHQ and include faces of different ages and genders. For the geometry, the 3D generation methods based on optimization (Magic123 and Dreamcraft3D) can't restore the stereoscopic shape of the human head. This is because they use view-dependent diffusion to guide the optimization process based on the 3D-SDS, and it does not generalize well to in-the-wild face images. Wonder3D can generate basic human head shapes but generally suffers from overly flat facial features in side views, and the facial surface lacks geometry detail. Besides, Panohead produces strange protrusions in the eye area. In contrast, our method, after introducing the identity information to the geometry sculpting stage, can restore fine geometry on the face while ensuring a high-quality overall head shape. For texture results, although Dreamcraft3D and Wonder3D can generate high-quality textures from the reference viewpoint, Dreamcraft3D, due to poor head geometry, is completely unable to generate images of the head from other angles. Wonder3D's

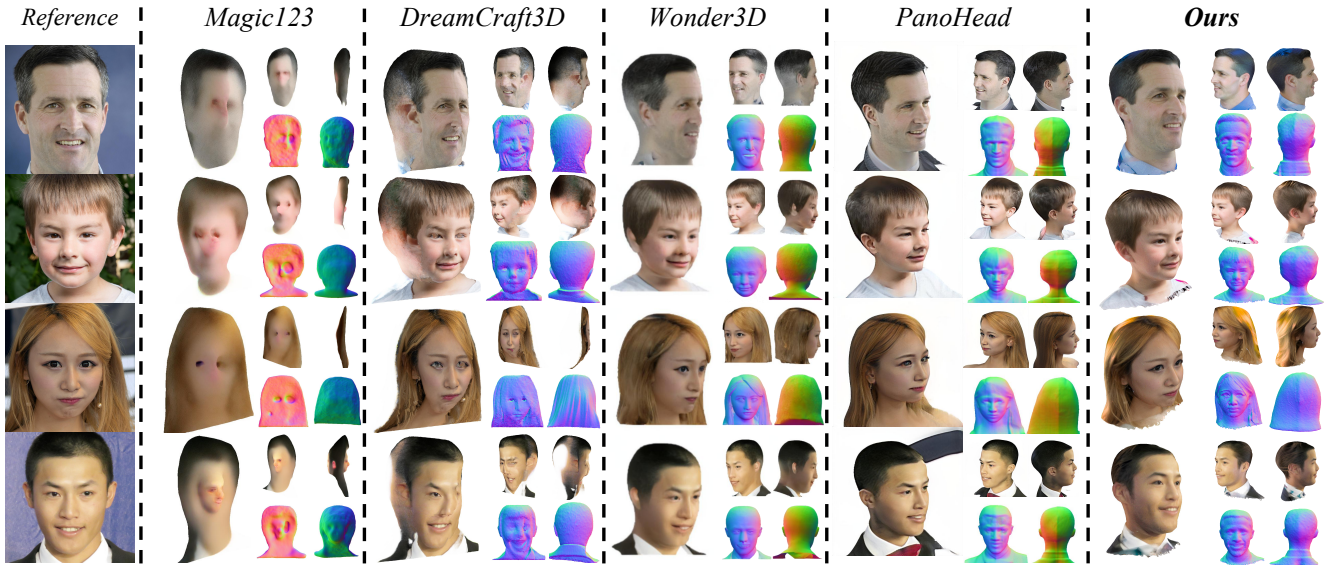


Figure 5. Qualitative evaluation with image-to-3D methods. Our method surpasses previous approaches in terms of the facial detail in head geometry as well as the realism of the texture.

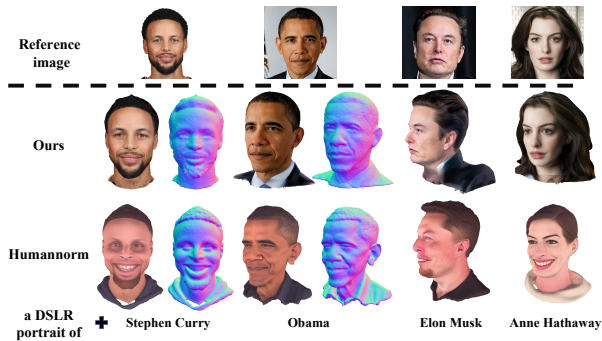


Figure 6. Qualitative evaluation with text-to-head method. Our method has a clear advantage in the realism of geometry and texture.

texture quality drops significantly on the side (i.e., the side rear view of the head in the first row of Wonder3D) and cannot produce high-resolution textures. Our method, after using ID-enhanced inpainting and refinement processes, can generate more photorealistic textures. In summary, our method can produce high-quality head geometry and realistic textures while fully restoring the facial information from the reference images.

**Qualitative evaluation with text-to-head method.** In Fig. 6, we show a comparison of our method with the current state-of-the-art text-to-head method Humannorm. Since text-to-human head methods can only accept text as input and cannot fully describe in-the-wild face information, the generated head may not match the face in the reference image. Therefore, for a fairer comparison, we choose exam-

ples of celebrities so that the text-to-head method can accurately generate heads based on the celebrity names. For generated geometry, Humannorm tends to generate heads with exaggerated structures, whereas our method generates far more realistic geometries. In terms of texture, due to the use of SDS loss to optimize the texture, the heads generated by Humannorm often have over-saturated colors. In contrast, our method fully utilizes both the reference image information and the identity information of the person depicted to generate more realistic faces.

### 5.3. Quantitative Evaluation

For each generated head model, we render images from five consistent viewpoints: left-frontal, left, right-frontal, right, and rear. All five rendered images are included in computing the CLIP-I and LPIPS metrics alongside the reference image. In the calculation of the ID metric, we compute the average Adaface [18] cosine similarity score across the four viewpoints excluding the rear. Note that if facial landmarks cannot be detected in an image from a particular viewpoint, its score is set to 0. In Tab. 1, we present the quantitative comparisons with the previous SOTA methods. Our method significantly outperforms previous approaches in terms of the ID metric, indicating its effectiveness in capturing the facial features of individuals and demonstrating high identity consistency across various perspectives in the analysis of novel viewpoints.

**User Study.** To validate our model’s robustness and quality, we conducted a user study with 15 random examples. Participants ranked five methods’ outputs based on quality from two random viewpoints. Our model ranked highest on

Table 1. Quantitative comparisons on head generation task.

Methods	LPIPS ↓	CLIP-I ↑	ID ↑	User Study ↑
Magic123	0.5601	0.4447	0.0245	1.11
PanoHead	<b>0.4343</b>	0.6600	<u>0.2737</u>	<u>4.09</u>
Wonder3D	0.5095	<b>0.6860</b>	0.2729	3.13
DreamCraft3D	0.4941	0.6074	0.2526	1.95
Portrait3D (Ours)	<u>0.4727</u>	<u>0.6605</u>	<b>0.4451</b>	<b>4.72</b>

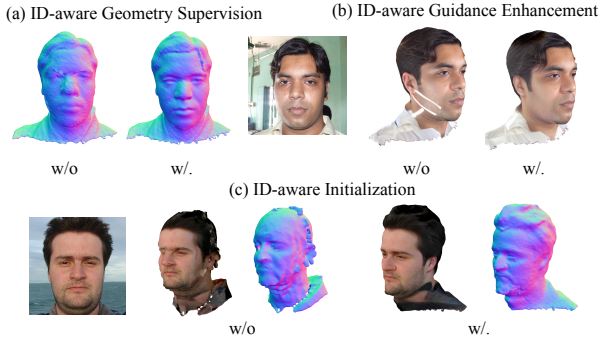


Figure 7. Visual ablation result of our ID-aware Initialization and Guidance.



Figure 8. Visual ablation result of our ID-Consistent Texture Inpainting and Refinement. Our method effectively reduces the artifact in texture generation.



Figure 9. 3D head with different styles. With the stylized diffusion model, we can achieve diversified stylized 3D head generation while maintaining identity.

average across 480 responses from 32 participants, confirming its superior quality.

#### 5.4. Ablation Study

##### Effectiveness of ID-aware Initialization and Guidance.

We present the visual in Fig.7 result to show the effectiveness of our ID-aware Initialization and Guidance method. (a) By replacing the normal map obtained through ID-aware Geometry Supervision with the normal map extracted from DPT[34, 35], we can observe that without ID-aware Ge-

ometry Supervision, the generated geometry loses many facial details. (b) When removing the ID-aware Guidance Enhancement in the texture generation stage, we can see that the faces lose the constraints imposed by identity information and easily produce artifacts for large angles (e.g., side faces) without sufficient reference image information. (c) We compare our ID-aware Initialization results with the use of Flame as the initialization geometry. As Flame aligns only with the facial landmarks, the head portions other than the face in the in-the-wild images are difficult to align with the initialization geometry, leading to difficulty in optimizing the geometry.

##### Effectiveness of ID-Consistent Texture Inpainting and Refinement.

As shown in Fig.8, without (a) Texture refinement stage, relying solely on inpainting can lead to discontinuous boundaries between each inpainting step, which is particularly noticeable at the intersection of the ears and hair. Additionally, if we do not adopt (b) Progressive Inpainting to complete the texture, but instead use a view-surrounding approach, incoherent texture colors will be generated (e.g. yellow part at the neck).

#### 5.5. Application

##### ID-consistent Texture Stylization.

With the powerful capability of text-to-image diffusion models, using stylized stable diffusion versions, we can modify the text prompt during the texture generation stage to achieve stylized 3D head generation. Due to the use of ID-aware guidance in the texture generation stage, the stylized heads generated can maintain the identity information of the character in the portrait image, as shown in Fig. 9.

#### 6. CONCLUSION

We propose Portrait3D, a novel method to realize 3D head generation from a single in-the-wild portrait image. By adding identity knowledge to the initialization, guidance, and geometry supervision part of the optimization process, our method significantly improves ID consistency and geometric details. Moreover, we design a two-stage ID-consistent texture inpainting and refinement method, which leads to coherent and photo-realistic head texture. Portrait3D outperforms previous methods in both geometry and texture quality, demonstrating the ability to generate high-fidelity 3D heads. These advantages combined with stylized 3D head generation bring great help for personalized 3D head asset generation.

##### Limitations and future work.

Although we can generate 3D human heads from portrait images, currently these 3D heads cannot be driven for tasks such as 3D talking avatars. In the future, we will attempt to develop drivable 3D human head generation methods.

## References

- [1] Sizhe An, Hongyi Xu, Yichun Shi, Guoxian Song, Umit Y Ogras, and Linjie Luo. Panohead: Geometry-aware 3d full-head synthesis in 360deg. In *Proceedings of the IEEE/CVF Conference on Computer Vision and Pattern Recognition*, pages 20950–20959, 2023. [3](#), [4](#), [7](#), [1](#), [2](#)
- [2] Ziqian Bai, Feitong Tan, Zeng Huang, Kripasindhu Sarkar, Danhang Tang, Di Qiu, Abhimitra Meka, Ruofei Du, Mingsong Dou, Sergio Orts-Escolano, et al. Learning personalized high quality volumetric head avatars from monocular rgb videos. In *Proceedings of the IEEE/CVF Conference on Computer Vision and Pattern Recognition*, pages 16890–16900, 2023. [2](#)
- [3] Eric R Chan, Connor Z Lin, Matthew A Chan, Koki Nagano, Boxiao Pan, Shalini De Mello, Orazio Gallo, Leonidas J Guibas, Jonathan Tremblay, Sameh Khamis, et al. Efficient geometry-aware 3d generative adversarial networks. In *Proceedings of the IEEE/CVF conference on computer vision and pattern recognition*, pages 16123–16133, 2022. [3](#)
- [4] Eric R Chan, Koki Nagano, Matthew A Chan, Alexander W Bergman, Jeong Joon Park, Axel Levy, Miika Aittala, Shalini De Mello, Tero Karras, and Gordon Wetzstein. Generative novel view synthesis with 3d-aware diffusion models. In *Proceedings of the IEEE/CVF International Conference on Computer Vision*, pages 4217–4229, 2023. [3](#)
- [5] Rui Chen, Yongwei Chen, Ningxin Jiao, and Kui Jia. Fantasia3d: Disentangling geometry and appearance for high-quality text-to-3d content creation. In *Proceedings of the IEEE/CVF International Conference on Computer Vision*, pages 22246–22256, 2023. [2](#), [3](#), [6](#)
- [6] Jiankang Deng, Jia Guo, Niannan Xue, and Stefanos Zafeiriou. Arcface: Additive angular margin loss for deep face recognition. In *Proceedings of the IEEE/CVF conference on computer vision and pattern recognition*, pages 4690–4699, 2019. [5](#)
- [7] Ainaz Eftekhari, Alexander Sax, Jitendra Malik, and Amir Zamir. Omnidata: A scalable pipeline for making multi-task mid-level vision datasets from 3d scans. In *Proceedings of the IEEE/CVF International Conference on Computer Vision*, pages 10786–10796, 2021. [5](#)
- [8] Yao Feng, Haiwen Feng, Michael J. Black, and Timo Bolkart. Learning an animatable detailed 3D face model from in-the-wild images. 2021. [4](#)
- [9] Guy Gafni, Justus Thies, Michael Zollhofer, and Matthias Nießner. Dynamic neural radiance fields for monocular 4d facial avatar reconstruction. In *Proceedings of the IEEE/CVF Conference on Computer Vision and Pattern Recognition*, pages 8649–8658, 2021. [3](#)
- [10] Philip-William Grassal, Malte Prinzler, Titus Leistner, Carsten Rother, Matthias Nießner, and Justus Thies. Neural head avatars from monocular rgb videos. In *Proceedings of the IEEE/CVF Conference on Computer Vision and Pattern Recognition*, pages 18653–18664, 2022. [2](#), [3](#)
- [11] Jianzhu Guo, Xiangyu Zhu, Yang Yang, Fan Yang, Zhen Lei, and Stan Z Li. Towards fast, accurate and stable 3d dense face alignment. In *Proceedings of the European Conference on Computer Vision (ECCV)*, 2020. [5](#), [1](#)
- [12] Yuan-Chen Guo, Ying-Tian Liu, Ruizhi Shao, Christian Laforte, Vikram Voleti, Guan Luo, Chia-Hao Chen, Zi-Xin Zou, Chen Wang, Yan-Pei Cao, and Song-Hai Zhang. threestudio: A unified framework for 3d content generation. <https://github.com/threestudio-project/threestudio>, 2023. [7](#)
- [13] Xiao Han, Yukang Cao, Kai Han, Xiatian Zhu, Jiankang Deng, Yi-Zhe Song, Tao Xiang, and Kwan-Yee K Wong. Headsculpt: Crafting 3d head avatars with text. *Advances in Neural Information Processing Systems*, 36, 2024. [2](#), [3](#), [4](#), [7](#), [1](#)
- [14] Yue Han, Jiangning Zhang, Junwei Zhu, Xiangtai Li, Yanhao Ge, Wei Li, Chengjie Wang, Yong Liu, Xiaoming Liu, and Ying Tai. A generalist facex via learning unified facial representation. *arXiv preprint arXiv:2401.00551*, 2023. [2](#)
- [15] Edward J Hu, Yelong Shen, Phillip Wallis, Zeyuan Allen-Zhu, Yuanzhi Li, Shean Wang, Lu Wang, and Weizhu Chen. Lora: Low-rank adaptation of large language models. *arXiv preprint arXiv:2106.09685*, 2021. [4](#)
- [16] Xin Huang, Ruizhi Shao, Qi Zhang, Hongwen Zhang, Ying Feng, Yebin Liu, and Qing Wang. Humannorm: Learning normal diffusion model for high-quality and realistic 3d human generation. *arXiv preprint arXiv:2310.01406*, 2023. [2](#), [3](#), [4](#), [5](#), [7](#)
- [17] Tero Karras, Samuli Laine, and Timo Aila. A style-based generator architecture for generative adversarial networks. In *Proceedings of the IEEE/CVF conference on computer vision and pattern recognition*, pages 4401–4410, 2019. [7](#)
- [18] Minchul Kim, Anil K Jain, and Xiaoming Liu. Adaface: Quality adaptive margin for face recognition. In *Proceedings of the IEEE/CVF conference on computer vision and pattern recognition*, pages 18750–18759, 2022. [8](#)
- [19] Tobias Kirschstein, Shenhan Qian, Simon Giebenhain, Tim Walter, and Matthias Nießner. Nersemble: Multi-view radiance field reconstruction of human heads. *ACM Transactions on Graphics (TOG)*, 42(4):1–14, 2023. [2](#)
- [20] Junnan Li, Dongxu Li, Silvio Savarese, and Steven Hoi. Blip-2: Bootstrapping language-image pre-training with frozen image encoders and large language models. In *International conference on machine learning*, pages 19730–19742. PMLR, 2023. [5](#)
- [21] Chen-Hsuan Lin, Jun Gao, Luming Tang, Towaki Takikawa, Xiaohui Zeng, Xun Huang, Karsten Kreis, Sanja Fidler, Ming-Yu Liu, and Tsung-Yi Lin. Magic3d: High-resolution text-to-3d content creation. In *Proceedings of the IEEE/CVF Conference on Computer Vision and Pattern Recognition*, pages 300–309, 2023. [2](#), [3](#)
- [22] Hongyu Liu, Xuan Wang, Ziyu Wan, Yujun Shen, Yibing Song, Jing Liao, and Qifeng Chen. Headartist: Text-conditioned 3d head generation with self score distillation. *arXiv preprint arXiv:2312.07539*, 2023. [2](#), [3](#), [7](#), [1](#)
- [23] Ruoshi Liu, Rundi Wu, Basile Van Hoorick, Pavel Tokmakov, Sergey Zakharov, and Carl Vondrick. Zero-1-to-3: Zero-shot one image to 3d object. In *Proceedings of the IEEE/CVF International Conference on Computer Vision*, pages 9298–9309, 2023. [2](#), [4](#)
- [24] Yuan Liu, Cheng Lin, Zijiao Zeng, Xiaoxiao Long, Lingjie Liu, Taku Komura, and Wenping Wang. Syncdreamer: Gen-

- erating multiview-consistent images from a single-view image. *arXiv preprint arXiv:2309.03453*, 2023.
- [25] Xiaoxiao Long, Yuan-Chen Guo, Cheng Lin, Yuan Liu, Zhiyang Dou, Lingjie Liu, Yuexin Ma, Song-Hai Zhang, Marc Habermann, Christian Theobalt, et al. Wonder3d: Single image to 3d using cross-domain diffusion. *arXiv preprint arXiv:2310.15008*, 2023. 4, 7, 2
- [26] Luke Melas-Kyriazi, Iro Laina, Christian Rupprecht, and Andrea Vedaldi. Realfusion: 360deg reconstruction of any object from a single image. In *Proceedings of the IEEE/CVF conference on computer vision and pattern recognition*, pages 8446–8455, 2023. 2
- [27] Jacob Munkberg, Jon Hasselgren, Tianchang Shen, Jun Gao, Wenzheng Chen, Alex Evans, Thomas Müller, and Sanja Fidler. Extracting triangular 3d models, materials, and lighting from images. In *Proceedings of the IEEE/CVF Conference on Computer Vision and Pattern Recognition*, pages 8280–8290, 2022. 2
- [28] Keunhong Park, Utkarsh Sinha, Jonathan T Barron, Sofien Bouaziz, Dan B Goldman, Steven M Seitz, and Ricardo Martin-Brualla. Nerfies: Deformable neural radiance fields. In *Proceedings of the IEEE/CVF International Conference on Computer Vision*, pages 5865–5874, 2021. 2
- [29] Gan Pei, Jiangning Zhang, Menghan Hu, Guangtao Zhai, Chengjie Wang, Zhenyu Zhang, Jian Yang, Chunhua Shen, and Dacheng Tao. Deepfake generation and detection: A benchmark and survey. *arXiv preprint arXiv:2403.17881*, 2024. 2
- [30] Ben Poole, Ajay Jain, Jonathan T Barron, and Ben Mildenhall. Dreamfusion: Text-to-3d using 2d diffusion. *arXiv preprint arXiv:2209.14988*, 2022. 2, 3
- [31] Guocheng Qian, Jinjie Mai, Abdullah Hamdi, Jian Ren, Aliaksandr Siarohin, Bing Li, Hsin-Ying Lee, Ivan Skokhodov, Peter Wonka, Sergey Tulyakov, et al. Magic123: One image to high-quality 3d object generation using both 2d and 3d diffusion priors. *arXiv preprint arXiv:2306.17843*, 2023. 3, 4, 7, 2
- [32] Aditya Ramesh, Mikhail Pavlov, Gabriel Goh, Scott Gray, Chelsea Voss, Alec Radford, Mark Chen, and Ilya Sutskever. Zero-shot text-to-image generation. In *International conference on machine learning*, pages 8821–8831. Pmlr, 2021. 2
- [33] Aditya Ramesh, Pratul Dhariwal, Alex Nichol, Casey Chu, and Mark Chen. Hierarchical text-conditional image generation with clip latents. *arXiv preprint arXiv:2204.06125*, 1(2):3, 2022. 2
- [34] René Ranftl, Katrin Lasinger, David Hafner, Konrad Schindler, and Vladlen Koltun. Towards robust monocular depth estimation: Mixing datasets for zero-shot cross-dataset transfer. *IEEE Transactions on Pattern Analysis and Machine Intelligence (TPAMI)*, 2020. 6, 9
- [35] René Ranftl, Alexey Bochkovskiy, and Vladlen Koltun. Vision transformers for dense prediction. *ArXiv preprint*, 2021. 6, 9
- [36] Daniel Roich, Ron Mokady, Amit H Bermano, and Daniel Cohen-Or. Pivotal tuning for latent-based editing of real images. *ACM Transactions on graphics (TOG)*, 42(1):1–13, 2022. 4
- [37] Robin Rombach, Andreas Blattmann, Dominik Lorenz, Patrick Esser, and Björn Ommer. High-resolution image synthesis with latent diffusion models. In *Proceedings of the IEEE/CVF conference on computer vision and pattern recognition*, pages 10684–10695, 2022. 2, 7
- [38] Chitwan Saharia, William Chan, Saurabh Saxena, Lala Li, Jay Whang, Emily L Denton, Kamyar Ghasemipour, Raphael Gontijo Lopes, Burcu Karagol Ayan, Tim Salimans, et al. Photorealistic text-to-image diffusion models with deep language understanding. *Advances in neural information processing systems*, 35:36479–36494, 2022. 2
- [39] Aditya Sanghi, Hang Chu, Joseph G Lambourne, Ye Wang, Chin-Yi Cheng, Marco Fumero, and Kamal Rahimi Malekshah. Clip-forge: Towards zero-shot text-to-shape generation. In *Proceedings of the IEEE/CVF Conference on Computer Vision and Pattern Recognition*, pages 18603–18613, 2022. 2
- [40] Tianchang Shen, Jun Gao, Kangxue Yin, Ming-Yu Liu, and Sanja Fidler. Deep marching tetrahedra: a hybrid representation for high-resolution 3d shape synthesis. In *Advances in Neural Information Processing Systems (NeurIPS)*, pages 6087–6101, 2021. 4, 6
- [41] Jingxiang Sun, Bo Zhang, Ruizhi Shao, Lizhen Wang, Wen Liu, Zhenda Xie, and Yebin Liu. Dreamcraft3d: Hierarchical 3d generation with bootstrapped diffusion prior. *arXiv preprint arXiv:2310.16818*, 2023. 3, 4, 7, 2
- [42] Junshu Tang, Tengfei Wang, Bo Zhang, Ting Zhang, Ran Yi, Lizhuang Ma, and Dong Chen. Make-it-3d: High-fidelity 3d creation from a single image with diffusion prior. In *Proceedings of the IEEE/CVF International Conference on Computer Vision*, pages 22819–22829, 2023. 2, 3
- [43] Can Wang, Menglei Chai, Mingming He, Dongdong Chen, and Jing Liao. Clip-nerf: Text-and-image driven manipulation of neural radiance fields. In *Proceedings of the IEEE/CVF Conference on Computer Vision and Pattern Recognition*, pages 3835–3844, 2022. 2
- [44] Zhengyi Wang, Cheng Lu, Yikai Wang, Fan Bao, Chongxuan Li, Hang Su, and Jun Zhu. Prolificdreamer: High-fidelity and diverse text-to-3d generation with variational score distillation. *Advances in Neural Information Processing Systems*, 36, 2024. 2, 3, 4, 6
- [45] Yuelang Xu, Benwang Chen, Zhe Li, Hongwen Zhang, Lizhen Wang, Zerong Zheng, and Yebin Liu. Gaussian head avatar: Ultra high-fidelity head avatar via dynamic gaussians. *arXiv preprint arXiv:2312.03029*, 2023. 3
- [46] Lior Yariv, Jiatao Gu, Yoni Kasten, and Yaron Lipman. Volume rendering of neural implicit surfaces. *Advances in Neural Information Processing Systems*, 34:4805–4815, 2021. 2
- [47] Hu Ye, Jun Zhang, Sibor Liu, Xiao Han, and Wei Yang. Ip-adapt: Text compatible image prompt adapter for text-to-image diffusion models. *arXiv preprint arXiv:2308.06721*, 2023. 5, 7
- [48] Wangbo Yu, Li Yuan, Yan-Pei Cao, Xiangjun Gao, Xiaoyu Li, Long Quan, Ying Shan, and Yonghong Tian. Hifi-123: Towards high-fidelity one image to 3d content generation. *arXiv preprint arXiv:2310.06744*, 2023. 3
- [49] Lvmin Zhang, Anyi Rao, and Maneesh Agrawala. Adding conditional control to text-to-image diffusion models. In

*Proceedings of the IEEE/CVF International Conference on Computer Vision*, pages 3836–3847, 2023. 5

- [50] Richard Zhang, Phillip Isola, Alexei A Efros, Eli Shechtman, and Oliver Wang. The unreasonable effectiveness of deep features as a perceptual metric. In *Proceedings of the IEEE conference on computer vision and pattern recognition*, pages 586–595, 2018. 4, 7
- [51] Mingwu Zheng, Haiyu Zhang, Hongyu Yang, and Di Huang. Neuface: Realistic 3d neural face rendering from multi-view images. In *Proceedings of the IEEE/CVF Conference on Computer Vision and Pattern Recognition (CVPR)*, pages 16868–16877, 2023. 2
- [52] Yufeng Zheng, Wang Yifan, Gordon Wetzstein, Michael J Black, and Otmar Hilliges. Pointavatar: Deformable point-based head avatars from videos. In *Proceedings of the IEEE/CVF conference on computer vision and pattern recognition*, pages 21057–21067, 2023. 2, 3

## Appendix

### A. Overview

In this supplementary material, we will show more content not mentioned in the main paper, including:

- More implementation details in our method.
- More ablation study.
- More visual results.
- More comparison results with previous methods.

### B. More implementation details

#### B.1. Align landmark with initialized geometry

In the geometry sculpting stage, landmarks can constrain the face layout in the generation process [13, 22], which effectively solves the multi-face Janus issue. Therefore, we need to obtain landmarks that are aligned with the initialized mesh to guide the geometry generation process.

We first use the face detector (3DDFA [11]) to obtain the 3D landmark of the face from the input image and get seven source keypoints as shown in Figure 10 (b). At the same time, the predicted camera extrinsic parameters are obtained, and this extrinsic component is aligned with the camera parameters in 3D GAN [1]. Next, utilizing the camera position, the imaging plane (blue plane), and the 3D coordinates of the key points on the imaging plane (red points on the blue plane), along with the initialized mesh, we employ the camera position as the origin of the rays (green rays). The directions of the rays are determined by the vectors from the camera position to the keypoints in the imaging plane. We use the Octree-accelerated ray-grid intersection method to compute the intersections of these rays with the initial mesh to obtain the target keypoints, as shown in Figure 10 (a). We then calculate the transformation matrix from the source keypoints to the target points to align the landmarks to the initialized mesh, as shown in Figure 10 (c).

#### B.2. Texture inpainting details

In the Progressive Texture Inpainting process, we set the camera trajectory to start from the front reference view, symmetrically select the viewpoint for inpainting, and gradually move the camera viewpoint to the back of the head. Specifically, the camera’s horizontal angle moves according to  $[0^\circ, 45^\circ, -45^\circ, 90^\circ, -90^\circ, 135^\circ, -135^\circ, 180^\circ]$ , and the vertical angle is set to  $-15^\circ$ . In this way, we are able to generate a coherent head texture.

#### B.3. Texture refinement details

In the texture refinement phase, in order to maintain the basic information of the initial texture and to eliminate the artifacts generated by inpainting, we add noise to the rendered image with a small timestep  $t = 120$  and denoise the

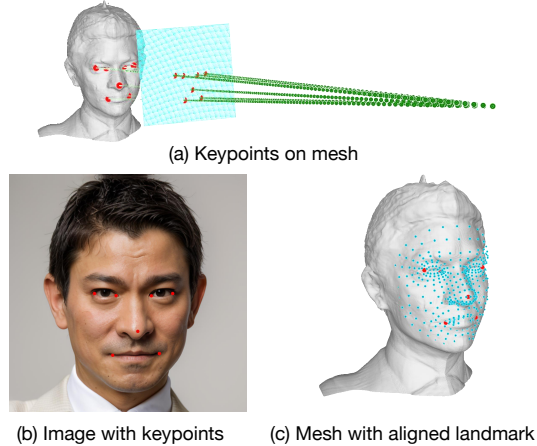


Figure 10. We compute the transformation matrix between source keypoints and target keypoints to align the landmark to the initialized mesh.

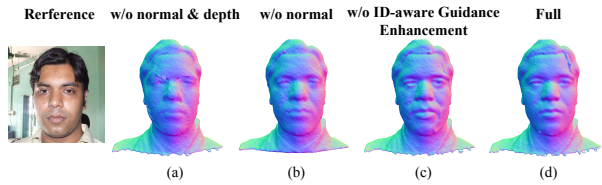


Figure 11. Visual result of ablation study. (a) Replace our ID-aware depth and normal with depth and normal predicted by DPT, (b) Geometry with only our ID-aware depth supervision, (c) Replace our ISD loss with SDS loss, (d) Our full method.

noised image with ID diffusion to generate a higher quality head texture. We employ the random camera sampling strategy with an elevation range of  $[-20^\circ, 45^\circ]$ , an azimuth range of  $[-180^\circ, 180^\circ]$ , a fovy range of  $[-30^\circ, 45^\circ]$ , and a camera distance range of  $[2.5, 4.0]$ .

### C. More ablation

In this section, we show the ablation result of our method in the geometry sculpting stage in Figure 11. (a) Without both ID-aware depth and normal supervision in reference view, the lack of depth results in a flatter head frontal geometry, and a flaky artifact in the geometry, (b) The absence of ID-aware normal map leaves the geometry lacking in detail, (c) Without employing the ID-aware Guidance Enhancement, uneven geometry may arise in the reference viewpoint. This is due to the inconsistency between the geometric supervision under the reference viewpoint and the guidance provided by the SDS. (d) Our full model can generate high-quality geometry compared to (a), (b) and (c).

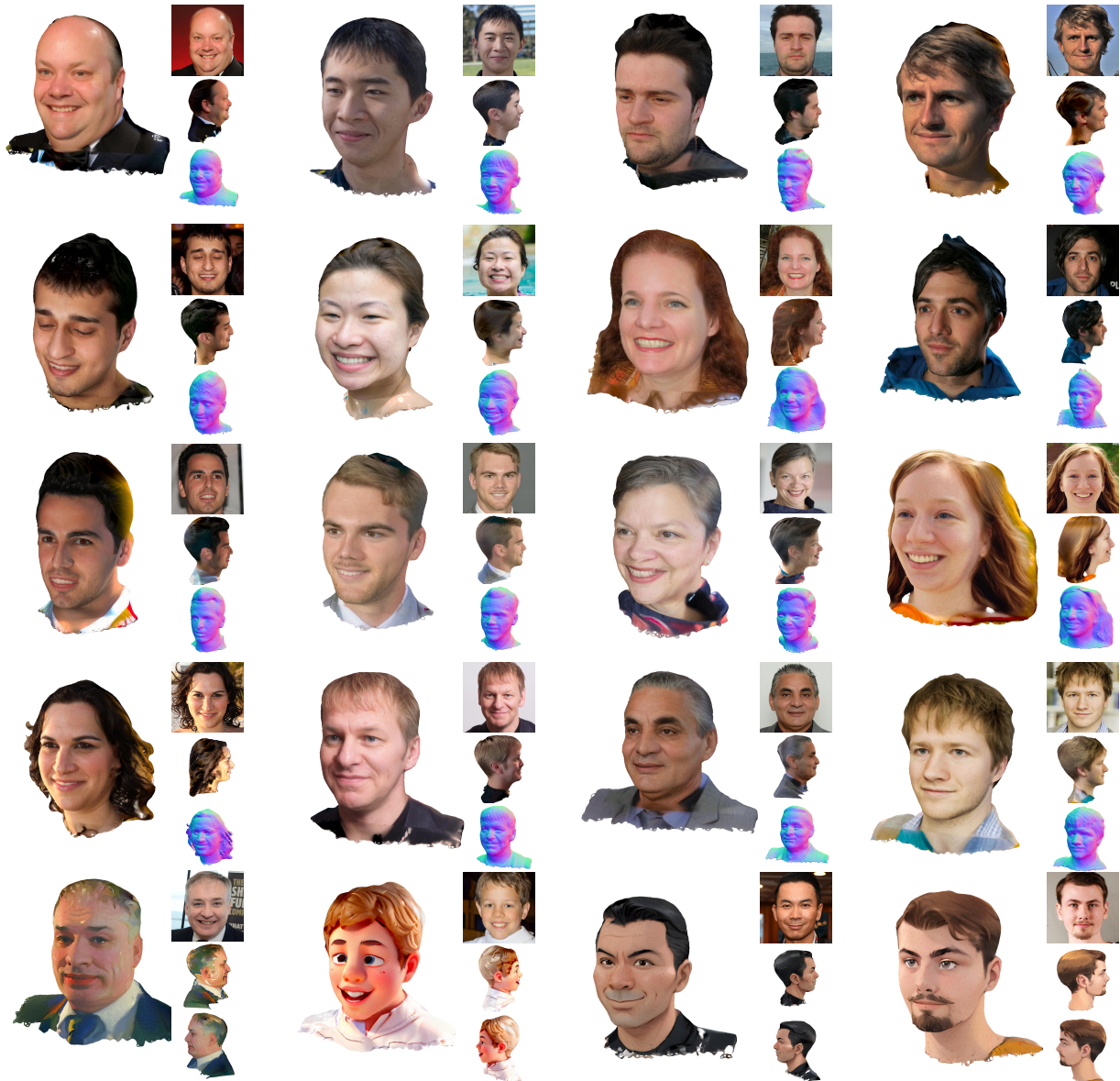


Figure 12. More visual result. Our method has high-quality geometry and photorealistic textures. Simultaneously, the generated 3D head models exhibit a high degree of consistency with the reference portrait images, showcasing the superior performance of our approach.

## D. More result

Figure 12 demonstrates the outstanding performance of our method in generating 3D head from a single in-the-wild portrait image. Our results exhibit high-quality geometry and photorealistic textures. Furthermore, by employing diverse stylized diffusion models, we are capable of generating stylized 3D heads while preserving the portrait’s identity.

## E. More comparison

We show more comparison of our method with previous methods in Figure 13. Compared with image-to-3D meth-

ods (Magic123 [31], Dreamcraft3D [41], wonder3D [25]), our method has better geometric and texture quality in side view and back view. Also, our method has better facial geometric details compared to Panohead [1].

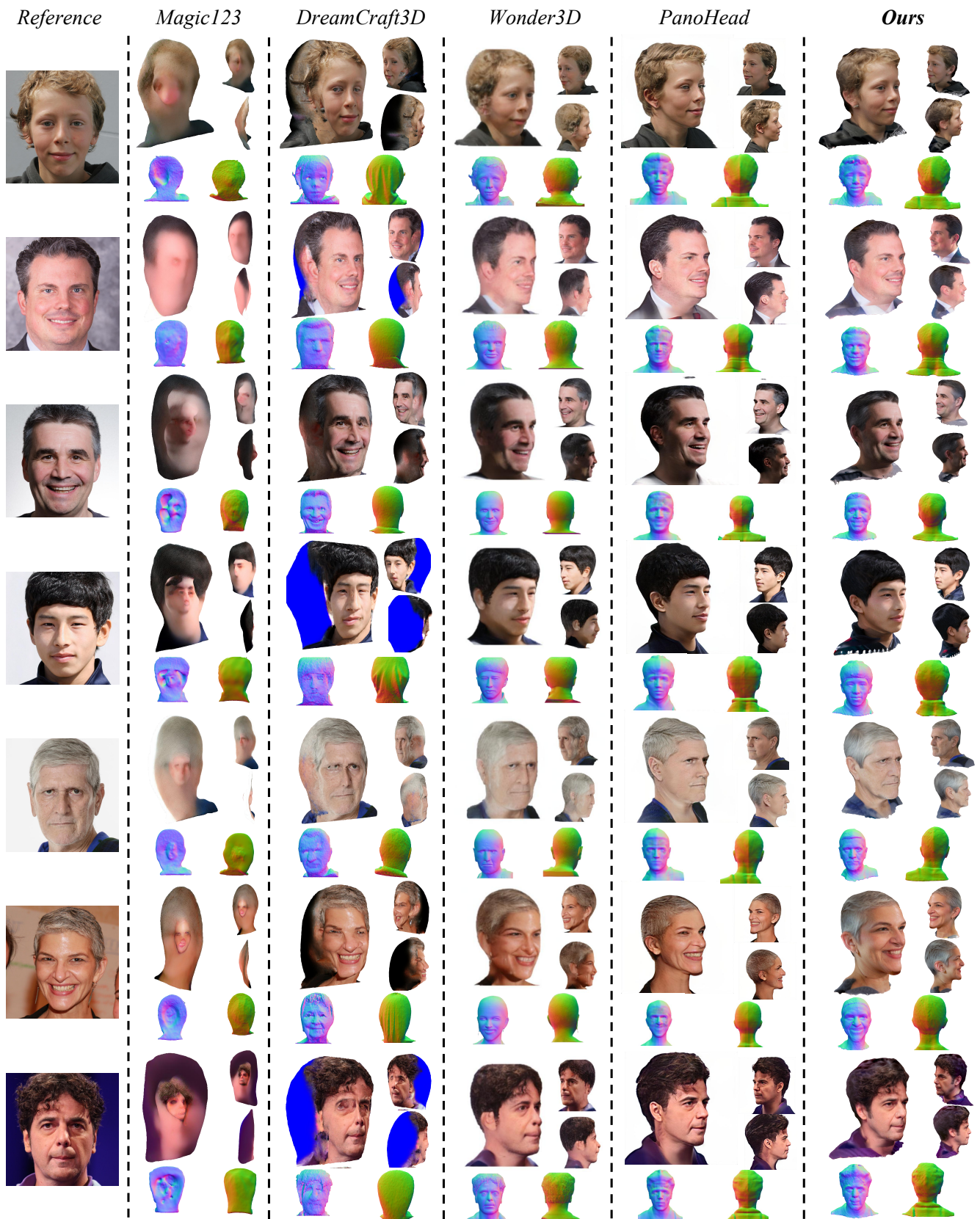


Figure 13. More comparison result. Compared to previous methods, our approach possesses more reasonable and richer geometry details, while maintaining photorealistic textures in both side and back views.